한국소음진동공학회논문집 제 13 권 제 5 호, pp. 400~408, 2003.

결함을 가진 증기발생기 U-튜브의 진동특성

Vibration Characteristics of Steam Generator U-tubes with Defect

조 종 철* · 정 명 조† · 김 웅 식* · 김 효 정* · 김 태 형**

Jong Chull Jo, Myung Jo Jhung, Woong Sik Kim, Hho Jung Kim and Tae Hyung Kim

(2003년 2월 25일 접수 ; 2003년 3월 19일 심사완료)

Key Words : Steam Generator(증기발생기), U-tube(U-튜브), Fluidelastic Instability(유체탄성 불안정성), Natural Frequency(고유진동수), Mode Shape(모드 형상), Through-wall Crack(관통 균열), Internal Pressure(내압)

ABSTRACT

This paper investigates the vibration characteristics of steam generator (SG) U-tubes with defect. The operating SG shell-side flow field conditions for determining the fluidelastic instability parameters such as added mass are obtained from three-dimensional SG flow calculation. Modal analyses are performed for the U-tubes either with axial or circumferential flaw with different sizes. Special emphases are on the effects of flaw orientation and size on the modal and instability characteristics of tubes, which are expressed in terms of the natural frequency, corresponding mode shape and stability ratio. Also, addressed is the effect of the internal pressure on the vibration characteristics of the tube.

1. Introduction

The problem of steam generator tube rupture (SGTR) at operating nuclear power plants has been addressed as one of the most significant safety issue worldwide for a long time. This is because the leakage due to SGTR has such serious implications as the potential for direct release of radioactive fission products to the environment and the loss of coolant.

Tube vibration excited by dynamic forces of external fluid flow in nuclear steam generators may either initiate such mechanical damages on intact tubes as fretting-wear and fatigue which may eventually result in severe tube failures or accelerate the growth of pre-existing flaw or crack caused by stress corrosion in the tubes. Even less significant dynamic forces of external fluid flow exerting to tube which can not cause any damage to the intact tube may lead to excessive vibration resulting in fatigue failure of the tube with flaw (crack) which is pre-existed or growing due to stress-corrosion. Therefore, with regard to nuclear safety, it is very important to assess the potential for SG tube failures due to fluidelastic instability to take the necessary preventive measures for minimizing the probability of SG tube failures in operating plants. The assessment of the potential for such a SG tube failure can be accomplished by performing the fluidelastic instability analysis for susceptible tube, for which the prerequisite is the performances of three-dimensional SG flow field

† 책임저자, 정회원, 한국원자력안전기술원 원자력안전연구실
E-mail : mjj@kins.re.kr
Tel : (042) 868-0467, Fax : (042) 868-0457
* 한국원자력안전기술원 규제기술연구부
** 한국전력기술주식회사 구조해석분야

calculation and tube modal analysis.

This study investigates the fluidelastic instability characteristics of steam generator U-tubes with defect. The operating SG shell-side flow field conditions for determining the fluidelastic instability parameters such as damping ratio and added mass are obtained from three-dimensional SG flow calculation using the ATHOS3 code. Modal analyses are performed for the finite element modelings of U-tubes either with axial or circumferential flaw with different sizes. The effects of flaw orientation and size on the modal and instability characteristics of tubes, which are expressed in terms of the natural frequency, corresponding mode shape and stability ratio, are investigated by comparing the calculations for the affected tubes to those for the intact tubes. Also, addressed in this paper is the effect of the internal pressure on the vibration characteristics of the tube.

2. Analysis

2.1 Thermal Hydraulic Analysis

One of the major prerequisites to the assessment is a detailed knowledge of the secondary side flow distributions along the tubes, which can be determined from a three dimensional two-phase thermal-hydraulic analysis for SGs. Several currently-used pressurized water reactor SG thermal-hydraulics codes are identified and among them ATHOS3[1] is one of the most widely used codes in the industry for three-dimensional thermal-hydraulic analysis of SGs, which is known to be a well documented and validated code.

Normal-to-tube cross flow gap velocity and density distributions over entire length of a specific U-tube can be obtained from the ATHOS3 calculation results. Typical results indicating non-uniform flow distributions in the U-bend region clearly illustrate the flow and heat transfer unbalance between hot and cold sides in U-tubes.

Two dominant dynamic parameters in the fluidelastic instability analysis of SG tubes are the distribution of effective (total) mass per unit length of the tube and the damping ratio. The distribution of effective mass per unit length of a specified tube would be determined from the following equation:

$$m_e(x) = m_t(x) + m_{pf}(x) + m_a(x) \quad (1)$$

where m and x are mass per unit length of tube and the distance along the tube length from the upper surface of tube sheet, respectively. The subscripts of m in equation (1), e, t, pf and a denote effective, tube metal, primary fluid and added mass, respectively.

The added (hydrodynamic) mass m_a is defined as the equivalent mass of external fluid vibrating with the tube, which increases the effective mass of the tube in a fluid.[2] The added mass of tube in a fluid may be calculated by either using the computer program AMASS[3] based on the analysis or the utilization of a semi-empirical correlation[4] based on the homogeneous two-phase density and on the equivalent diameter representing the confinement due to surrounding tubes.

It is very important to understand the damping mechanisms of SG U-tubes in the flow-induced vibration analysis. However, damping is difficult to predict because it depends on geometrical conditions of tubes and their supports, flow conditions, non-linear effects and the multiplicity of energy dissipation mechanisms for multi-span SG tubes. Damping ratio of tubes in liquids may be determined either from available measured data of Pettigrew et al.[5] or by the empirical expressions for the viscous and support damping suggested in the previous study of Pettigrew et al.[6]

The secondary side of a SG, especially the U-bend region, is actually a two-phase flow field. Damping in two-phase mixtures is known to be very different from that in liquids. Because of

much difficulty from an experimental point of view, little data on the damping of U-tubes in steam-water mixture flows are available at the present. The support damping of tubes in either liquids or two-phase mixtures is dominant so that a large percentage of the total damping energy is dissipated at the support.[4]

2.2 Modal Analysis

Modal analyses using a commercial computer code ANSYS 6.1[7] are performed to find the vibration characteristics of the U-tube. Three different kinds of finite element models for U-tube are developed ; full model, detailed one span model and simplified full model.

Full models, consisting of full U-tube, are modeled as elastic shell elements (SHELL63) with four nodes. The entire length of the U-tube is divided into 784 elements in the axial direction and 8 elements in the circumferential direction, and therefore the total number of elements used is 6272 as shown in Fig. 1. To see the defect effect on the frequencies, axial or circumferential through-wall crack is assumed in the lowest span in the hot side of the U-tube. The cracks are varied from 0 to 100 % in size in the axial and circumferential direction. They are simulated by merging the two nodes which are defined at the same location.

Detailed one span models, consisting of the lowest span in the hot side of the U-tube, are developed using 3-dimensional structural solid elements (SOLID45) defined by eight nodes having three degrees of freedom. The entire length of the one span is divided into 260 elements in the axial direction, 80 elements in the circumferential direction and 3 elements in the radial direction, and therefore the total number of elements used is 62400 as shown in Fig. 2. To see the defect effect on the frequencies, circumferential cracks are assumed in the inner or outer surface of the U-tube. The cracks are varied from 0 to 100 % in depth in the radial direction.

Finally, simplified full models are developed using the elastic straight pipe elements (PIPE16) for straight region and elastic curved pipe elements (PIPE18) for U-bend region. The U-tube consists of 62 PIPE16 elements in the straight region and 36 PIPE18 elements in the U-bend region as shown in Fig. 3 for four different types of U-tubes.

The boundary conditions at the tube sheet nodes are fixed but the nodes at tube sheet plates and anti-vibration bars are free to move in the axial direction.

The Block Lanczos method is used for the eigenvalue and eigenvector extractions to calculate 40 frequencies, which are composed of in-plane and out-of-plane modes.

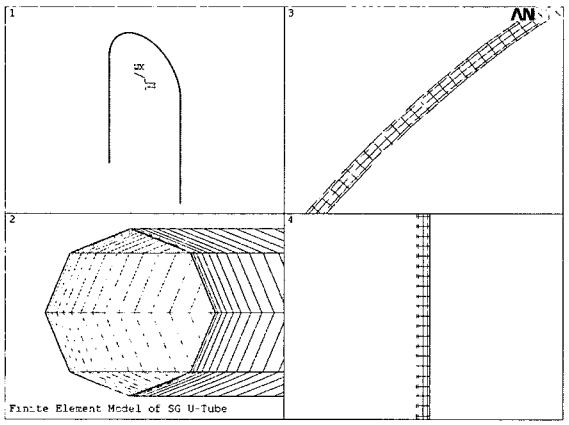

Fig. 1 Finite element model of U-tube

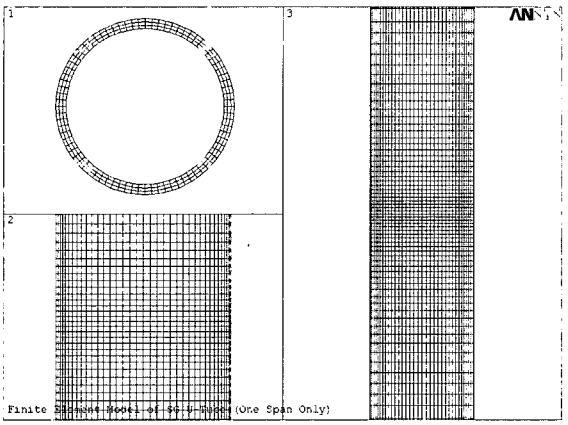

Fig. 2 Finite element model of detailed U-tube

2.3 Fluidelastic Instability Analysis

The critical velocity to initiate fluidelastic instability was originated by Connors[8] for the simple case of a tube bank subjected to uniform cross flow over the entire length of the tubes. The formulation of fluidelastic instability proposed by Connors is a semi-empirical correlation fitted by experimental data and is expressed in terms of a dimensionless flow velocity called a reduced velocity $V_{c,n}/f_n d$ and a dimensionless mass-damping parameter

$$V_{c,n}/f_n d = K(2\pi\zeta_t m_o/\rho_o d^2)^{0.5} \quad (2)$$

where $V_{c,n}$, K, f_n, ζ_1, m_o, ρ_0 and d are the critical velocity of the nth free vibration mode, the fluidelastic instability coefficient (or the Connors constant), the natural frequency of the nth mode, the total damping ratio, the total mass per unit length of the tube, the secondary fluid density and the outer diameter of tube, respectively.

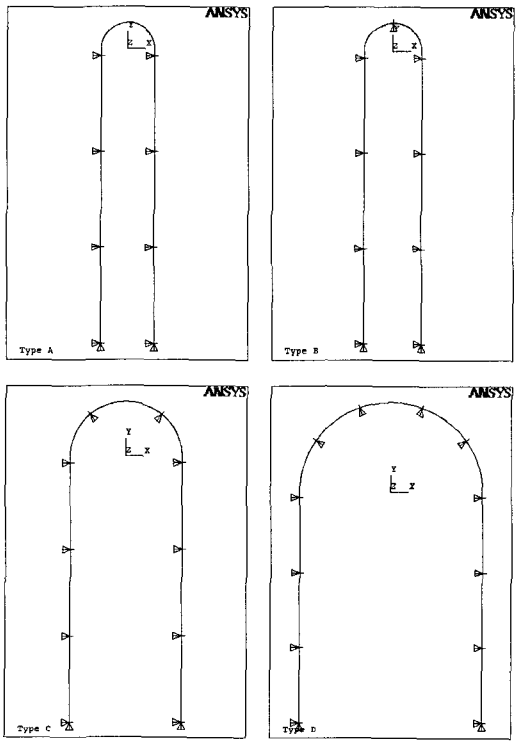

Fig. 3 Finite element models of U-tube by PIPE element

The fluidelastic instability coefficient K is a function of the tube arrangement and the ratio of tube pitch p over the outer diameter of tube d. The critical velocity $V_{c,n}$ is related to the gap velocity V_g between the tubes, which is determined based on the tube pitch and diameter as applied to the approach or free stream velocity V. The gap velocity determined using ATHOS3 in the fluid region is

$$V_g = \frac{p}{p-d} V_\infty \quad (3)$$

For most of practical shell-and-tube type heat exchangers including SGs, the tube bundles consist of multi-span tubes and only partial portions of the tubes may be exposed to cross flow. The onset of fluidelastic instability of multi-span tubes partially subjected to cross flow may be predicted by several approaches. It has been indicated that the equivalent velocity approach based on mode shapes is valid and the simplest one to use.[9] Equation (2) was originally extended by Eisinger and Juliano[10] for the use of equivalent velocity approach in the fluidelastic instability analysis for the tubes partially subjected to cross flow.

The fluidelastic instability for tubes partially exposed to cross flow can be evaluated by the comparison of the critical velocity $V_{c,n}$ with the effective cross flow gap velocity V_{ge} which is a uniform cross flow velocity equivalent to the actual non-uniform normal-to-tube cross flow gap velocity distribution along the tube length $V_g(x)$, where x denotes the distance along the tube with full length from the hot side tube end.

$V_{ge,n}$ is variable depending on the free vibration mode as in the case of $V_{c,n}$. The value of $V_{ge,n}$ equivalent to $V_g(x)$ can be determined by weighting the nth mode shape as follows:

$$V_{ge,n} = \frac{m_{eo}}{\rho_{eo}} \frac{\int_0^l \rho(x) V_g^{\,2}(x) \varphi_n^{\,2}(x) dx}{\int_0^l m_e(x) \varphi_n^{\,2}(x) dx} \quad (4)$$

where $\rho(x)$ and $\varphi_n(x)$ are the secondary fluid density distribution along the tube and the nth mode shape function, respectively.

The local normal-to-tube cross flow gap velocity along the tube length $V_g(x)$ can be determined from the ATHOS3 code calculated porosity-based intermediate velocity components.

The stability ratio $R_{s,n}$ is defined by the ratio of $V_{ge,n}$ over $V_{c,n}$ as given

$$R_{s,n} = V_{ge,n} / V_{c,n}, \; n = 1, 2, 3, \cdots \quad (5)$$

where $R_{s,n}$ indicates the stability ratio for the nth vibration mode.

The maximum value among the stability ratios for all vibration modes of a specified tube is used as the criteria to assess the potential instability of the tube. If the maximum value of stability ratio R_s is smaller than unity, the tube is fluidelastically stable. Otherwise, it is unstable and its vibration amplitude becomes divergent rapidly as R_s increases beyond unity.

3. Results and Discussion

The effective mass distribution along the entire tube is shown in Fig. 4, which was calculated from the thermal-hydraulic analysis. This mass density is used to find the vibration characteristics. The through-wall cracks are assumed in the lowest one span of the U-tube hot side. Various sizes of crack from 0 to 100 % in the axial and circumferential directions are considered. The frequency variations are shown in Figs. 5 and 6 with respect to the crack sizes. The frequency variations with crack sizes indicate that there are no frequency changes in the axial crack but some frequency changes in circumferential crack. Normalized frequencies of the tube with circumferential crack with respect to the tube without defect are also shown in Fig. 6, which

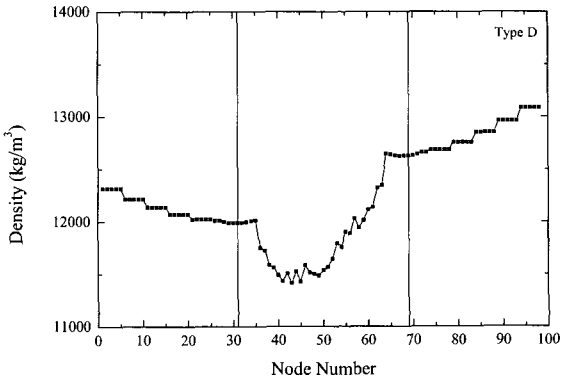

Fig. 4 Effective mass distribution along the U-tube

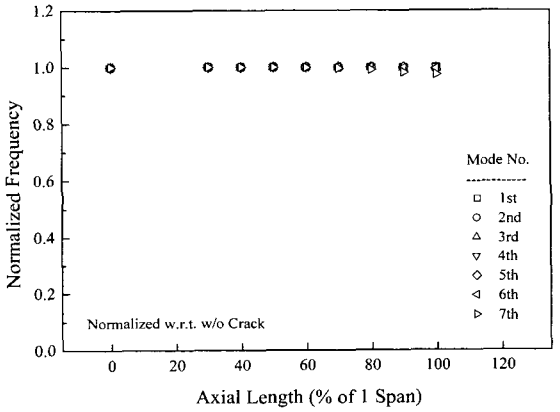

Fig. 5 Frequency variations with respect to axial through-wall crack length

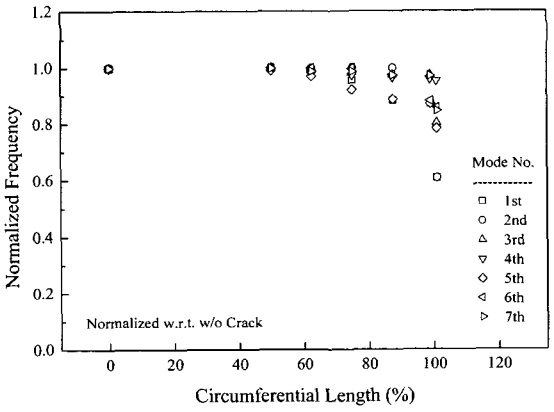

Fig. 6 Frequency variations with respect to circumferential through-wall crack length

indicates that frequencies begin to decrease when crack length becomes 270° in the circumferential direction.

From these results, detailed analyses are performed for the circumferential crack. Different depths of surface crack are considered from 0 (no crack) to 100 % (through-wall crack) and their frequencies are shown in Figs. 7 and 8. For the circumferential crack length of 360°, the radial depths are varied, but there are no significant changes of frequency until it propagates to penetration. Also, for the radial depth of 99.9 %, the circumferential crack lengths are varied, which generates the same results. All of these results

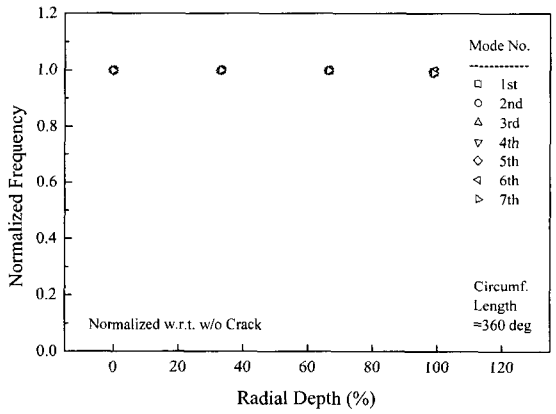

Fig. 7 Frequency variations with respect to radial depth for circumferential crack length = 360°

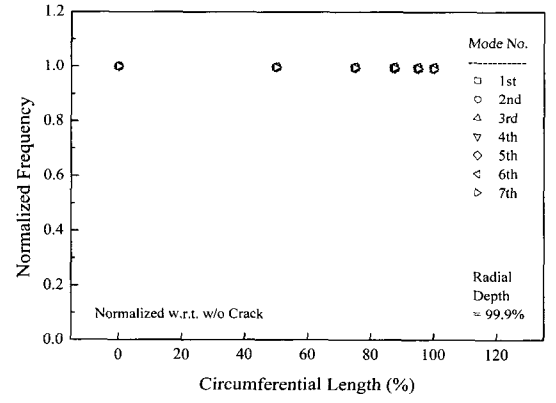

Fig. 8 Frequency variations with respect to circumferential length for radial depth = 99.9 %

show that the frequency changes are negligible even though there is a crack in the U-tube and it is not a through-wall crack.

To investigate the frequencies of the U-tube with inner and outer surface cracks, circumferential length of 360° cracks are assumed. Their results are compared in Table 1 and it is concluded that there are little changes in frequencies of the U-tube with inner and outer surface cracks.

Two different elements such as pipe and shell elements are used for the finite element analyses of the simplified U-tube modeling. In using shell elements the number of element in the circumferential direction increases from 8 to 40 and the resulting frequencies are compared to those of pipe elements as shown in Table 2. In this table,

Table 1 Frequency comparisons between detailed U-tube model with inner and outer surface crack

% Size (depth/thk)	Loc.	Frequency (Hz)				
		1st	2nd	3rd	4th	5th
33.3	Inner	43.6	140.7	292.0	495.8	750.0
	Outer	43.6	140.7	292.0	495.8	750.0
66.6	Inner	43.6	140.7	291.5	495.7	748.7
	Outer	43.5	140.7	291.3	495.6	748.1
99.9	Inner	43.3	140.5	289.2	495.0	743.0
	Outer	43.1	140.4	287.7	494.7	739.6
0	Intact	43.6	140.7	292.1	495.8	750.2

Table 2 Frequency comparisons between shell and pipe elements for U-tube without crack

No.	Element				
	Pipe	Shell			
		N*=8	N=16	N=32	N=40
1	32.24	30.57	31.76	32.07	32.11
2	32.25	30.60	31.79	32.10	32.14
3	33.14	31.42	32.65	32.97	33.00
4	33.80	32.09	33.34	33.66	33.70
5	42.92	40.73	42.31	42.72	42.77
6	43.29	40.98	42.59	43.01	43.06
7	44.69	42.34	44.00	44.43	44.48
8	46.52	44.18	45.88	46.32	46.37

*N = number of elements in the circumferential direction

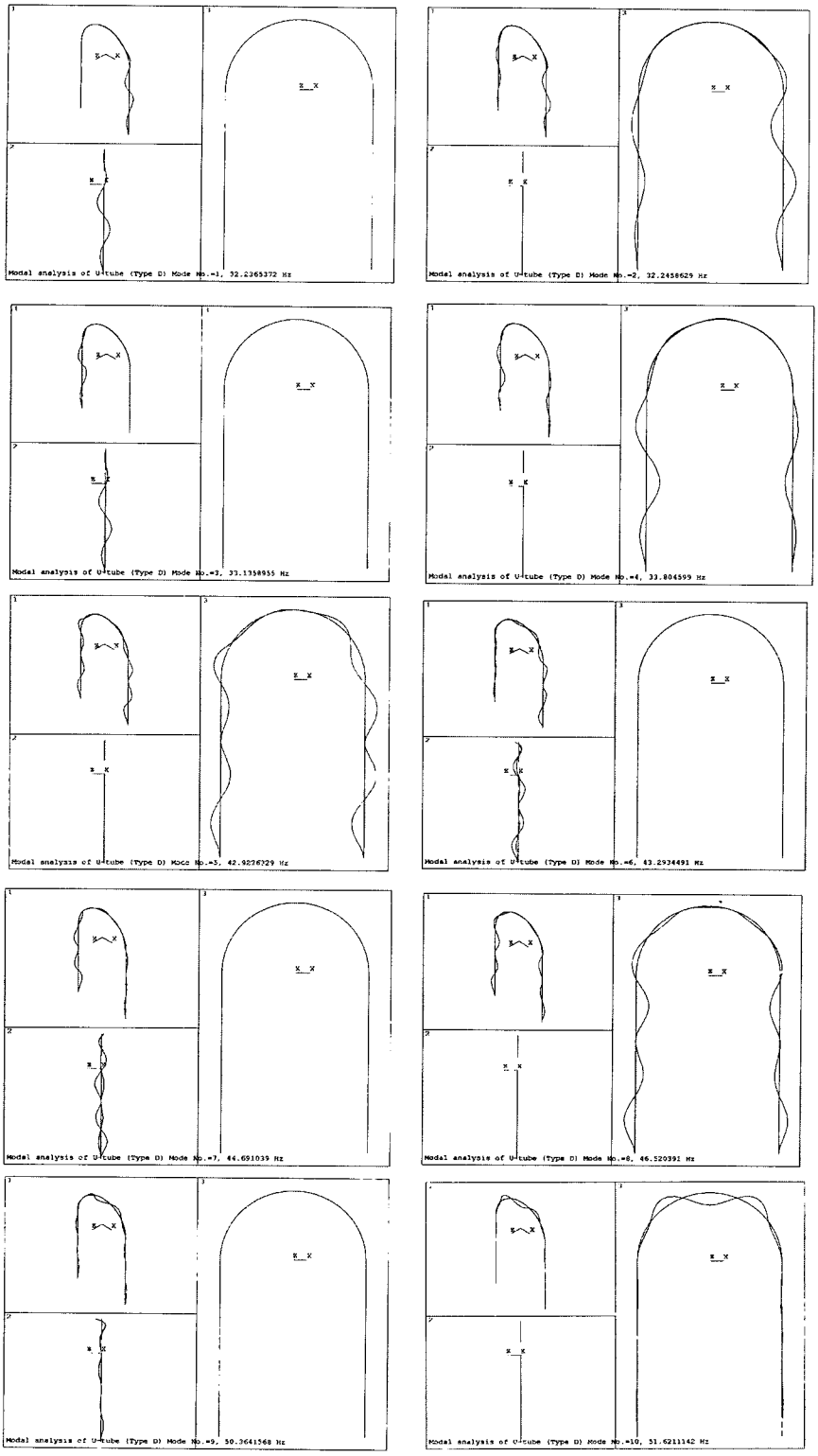

Fig. 9 Mode shapes of U-tube

the more number of shell elements, the resulting frequencies are getting closer to those of pipe elements. This is explained by the fact that total mass and moment of inertia which affect the natural frequencies of the structure are closer to those of pipe element as the number of shell elements increase as shown in Table 3.

Four different types of U-tubes for SG Model 51 are chosen to investigate the stability as shown in Table 4 because they are located in the higher cross-flow velocities as compared to the interior of the tube bundle. Modal analyses are performed and mode shapes consisting of in-plane and out-of-plane modes are shown in Fig. 9.

Table 3 Comparisons of total mass and moment of inertia between shell and pipe elements for U-tube without crack

No.	Element				
	Pipe	Shell			
		N*=8	N=16	N=32	N=40
mass	12.956	12.625	12.872	12.935	12.942
Ixx	37.62	36.69	37.41	37.59	37.61
Iyy	24.52	23.91	24.38	24.49	24.51
Izz	62.14	60.60	61.78	62.08	62.12
Ixy	0.2346	0.2286	0.2331	0.2342	0.2344

*N = number of elements in the circumferential direction

Table 4 Geometric description of tube bundle

Parameters	Type A	Type B	Type C	Type D
Outer diameter(10^{-2} m)	2.2225	2.2225	2.2225	2.2225
Inner diameter(10^{-2} m)	1.968	1.968	1.968	1.968
Thickness (10^{-3} m)	1.27	1.27	1.27	1.27
Radius of curvature of U-bend (m)	0.3458	0.3810	0.8041	1.5200
Number of tube support plates	7	7	7	7
Number of AVB support points in U-bend	0	1	2	4
Angle of curved spans (°)	0	90	50, 80	35, 40

To investigate the effect of the internal pressure on the vibration characteristics of the tube, pressures are input as surface loads on the elementsurfaces of Type D. The resulting normalized frequencies with respect to the without pressure case are shown in Fig. 10 with respect to the unpressurized pipe, which indicates that frequency changes are negligible up to the internal pressure of about 10 MPa. Above this pressure, frequency drops very rapidly with the increase of the pressure. The normalized frequencies can be represented for all modes as:

$$y = 148522\exp\left(\frac{-P}{3.9217E13}\right) - 148521 \tag{6}$$

where y and P are the normalized frequency and the internal pressure (Pa), respectively. When considering that pressure difference during normal operation of the nuclear power plant is almost 5 MPa, frequency difference can be concluded to be negligible with the inclusion of the internal pressure.

The results of velocity and fluid density variation versus tube span coordinates from thermal hydraulic analysis and tube normalized displacements from modal analysis are used to calculate the effective velocities of equation (4). Also, the critical velocities of equation (2) are

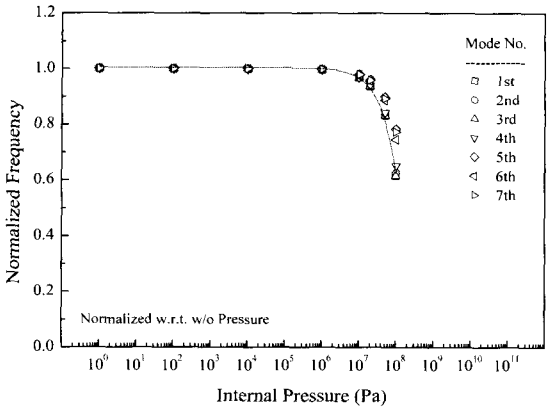

Fig. 10 Normalized frequency variations with respect to w/o internal pressure case

calculated from the tube geometries and natural frequencies, etc. Finally, stability ratios are determined for each mode from equation (5) and found to be less than unity. Therefore, no significant tube fretting or wear is expected as a result of fluid induced tube vibration.

4. Conclusions

To investigate the vibration characteristics of U-tube with defect, finite element models are developed for an assembly and one detailed span. Modal analyses for various sizes of axial and circumferential through-wall cracks and circumferential surface cracks are performed generating the following conclusions:

(1) For through-wall crack, circumferential crack is more severe than axial crack for frequency changes.

(2) Frequency changes are not much affected by the size and propagation of cracks, or there is little change in the frequency if the crack is not resulting in through-wall crack even though it is initiated and propagated. Therefore frequency change is negligible due to the propagation of a crack until through-wall crack.

(3) Frequencies of tube with outer surface crack are smaller than those with inner surface crack but the difference is negligible.

The frequency changes due to the defect were negligible unless cracks are propagated to through-wall penetration. Therefore the instability characteristics due to the existence of crack of the tube are not changed until it becomes through-wall penetration.

Also, frequency changes of the tube are negligible with the inclusion of the internal pressure during the normal operation and therefore it can be concluded that instability characteristics are not affected by the internal pressure of the tube.

References

(1) Keeton, L. W. and Singhal, A. K., 1986, "ATHOS3 : A Computer Program for Thermal Hydraulic Analysis of Steam Generators," EPRI Report NP-4604-CCM, Vols. 1~3.

(2) Jhung, M. J. and Jeong K. H., 2001, "Natural Vibration Analysis of Two Circular Plates Coupled with Bounded Fluid," 한국소음진동공학논문집, 제 11 권, 제 9 호, pp. 439~453.

(3) Chen, S. S. and Chung, H., 1976, "Design Guide for Calculating Hydrodynamic Mass, Part 1 : Circular Cylindrical Structures," ANL Report ANL-CT-76-45, Argonne, IL.

(4) Pettigrew, M. J., Taylor, C. E. and Kim, B. S., 1989, "Vibration of Tube Bundles in Two-phase Cross-flow : Part 1 Hydrodynamic Mass and Damping," ASME Journal of Pressure Vessel Technology, Vol. III, pp. 466~477.

(5) Pettigrew, M. J., Rogers, R. J. and Axisa, F., 1986, "Damping of Multi-span Heat Exchanger Tubes, Part 2 : In Liquids," ASME Publication PVP-Vol. 104, New York.

(6) Pettigrew, M. J., Carlucci, L. N., Taylor, C. E. and Fisher, N. J., 1991, "Flow-induced Vibration and Related Technologies in Nuclear Components," Nuclear Engineering and Design, Vol. 131, pp. 81~100.

(7) ANSYS, 2001, ANSYS Structural Analysis Guide, ANSYS, Inc., Houston.

(8) Corners, H. J., 1981, "Flow-induced Vibration and Wear of Steam Generator Tubes," Nuclear Technology, Vol. 55, pp. 311~331.

(9) Eisinger, F. L., Rao, M. S. M. and Steininger, D. A., 1989, "Numerical Simulation of Fluidelastic Instability of Multispan Tubes Partially Exposed to Crossflow," SMiRT-10, Vol. T, pp. 45~57.

(10) Eisinger, F. L. and Juliano, T. M., 1975, "Flow-induced Vibration Analysis of Recuperator Tube Bank," Foster Wheeler Energy Corp. Report 156-MA-75-48.